

Characterization of Coal Char Gasification Rate

Tadafumi Adschiri

Dept. of Biochemistry and Chemical Engineering, Tohoku University, Sendai 980, Japan

Takao Nozaki and Takehiko Furusawa

Dept. of Chemical Engineering, University of Tokyo, Tokyo 113, Japan

Zhu Zi-bin

Dept. of Chemical Engineering, East China University of Chemical Technology, May Road, China

The transient kinetic technique was applied to the evaluation of both elemental rate constants, k_{av} and k_{in} , and the amount of reactive carbons, n_w , which participate in gasification. The dynamic change in gasification rate with increasing conversion is due to the change in n_w . Differences in the gasification rates of ten different chars can be explained mostly by the differences in n_w , rather than by those of k_{av} or k_{in} . n_w increased and approached a maximum value, N , with increasing partial pressure of carbon dioxide. The maximum value, N , related closely to the carbon structure of char, especially to the crystallite size of graphite.

Introduction

Rational design and analyses of coal gasifier require sound understanding of gas-solid contact and accurate description of the gasification rate of coal char. It is well known that the gasification rates and the pressure dependence of them differ significantly.

Quite a few researchers have tried to explain differences in gasification rates by introducing parameters. Smith et al. (1978), Adschiri et al. (1985, 1986a,b), and Takeda et al. (1985) employed the surface area as a parameter for interpreting the difference of gasification rates. Kasaoka et al. (1982) correlated the gasification rates with the amount of water physically adsorbed at 303 K. Laine et al. (1963) introduced the active surface area (ASA), which was defined as the amount of chemisorbed oxygen at a low temperature. Some researchers (Mims and Pabst, 1983; Sams and Shadman, 1986; Saber et al., 1986; Cerfontain, 1986; Hashimoto et al., 1987) employed gasification agents (CO_2 and H_2O) for the adsorbate and succeeded in describing the correlation between the gasification rate and the evaluated ASA. Furthermore, Hashimoto et al. (1987) demonstrated that the molar ratio of alkali metals in char (Na and K) to the amount of adsorbed oxygen is around unity. Although the adsorption method and adsorption temperature for the evaluation of ASA differed among the researchers, ASA is regarded as a good parameter for the interpretation of the difference in gasification rate (Radovic et al., 1983, 1985; Hashimoto et al., 1986).

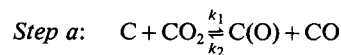
These approaches were based on the following assumptions:

1) gasification rate is described by the intrinsic rate constant, $k(T)$, and the number of active sites, N_T , as

$$\text{rate} = k(T) N_T \quad (1)$$

and 2) N_T is not affected by the temperature.

Recently, Freund (1985, 1986) introduced transient kinetics method to directly evaluate the rate constant without using any parameter for N_T , by assuming Ergun's mechanism (1956).



He evaluated the desorption rate constant, k_3 , from the transient decay of carbon monoxide concentration (step b) after shutting off the carbon dioxide stream (step a).

The authors of this article (Zhu et al., 1987, 1988, 1989; Nozaki et al., 1990) and Lizzio et al. (1990) applied this technique to evaluate the amount of surface oxide complex, n_w , from the same response, which was determined by measuring the integrated amount of carbon monoxide evolved after shutting off carbon dioxide. We used the term "working active site" for n_w by considering Ergun's mechanism, while Radovic's group (Lizzio et al., 1990; Jiang and Radovic, 1989) used the term "reactive surface area (RSA)." The amount of work-

Table 1. Ultimate and Proximate Analyses of Parent Coals

Coal	Ash	Volatile Matter	Fixed Carbon	C	H	N	S	O
	Wt. % Dry Base			Wt. % d.a.f.				
Hokutaku	23.1	46.8	30.1	68.7	4.8	1.4	0.5	24.6
Yallourn	0.7	45.4	53.9	69.8	4.2	0.6	0.2	25.2
Baiduri	5.3	42.8	51.9	71.3	4.9	1.4	1.1	21.4
Taiheiyo	21.4	42.7	35.9	77.0	6.2	1.2	—	15.6
Colowyo	5.6	39.6	54.8	77.3	5.1	1.6	0.4	15.6
Wandoan	8.2	45.8	46.1	78.2	5.9	0.9	0.4	14.7
Plateau	9.8	42.4	47.8	80.0	5.7	1.5	0.9	12.1
Ermelo	13.5	30.2	56.3	81.8	4.8	1.9	1.2	10.4
Datong	10.6	27.8	61.7	85.5	4.9	1.7	0.5	7.5
Hongei	7.1	6.6	86.3	92.7	3.7	1.0	0.4	2.3

ing active sites, n_w , was correlated closely to the gasification rate (Zhu et al., 1987, 1988, 1989; Lizzio et al., 1990; Jiang and Radovic, 1989). The present authors (1989, 1990) applied the transient kinetics method also for the evaluation of the rate constants, k_1 and k_3 . k_1 and k_3 were determined from the unsteady state variation of carbon monoxide concentration after introducing carbon dioxide. Thus, the characteristics of the transient kinetics method are independent evaluation of the rate constants, $k(T)$, and the number of reactive carbons, N_T .

In this study, both the rate constants and the amount of working active sites were evaluated for ten chars over wider ranges of temperature and pressure by using the transient kinetics method. Dependence of both factors on partial pressure of carbon dioxide were also evaluated. The primary objective of the present study is to demonstrate the validity of this method; the second is to interpret the difference among gasification rates of chars based on the obtained results; and the third is to find out the relation between these factors and the carbon structure of char.

Experimental Studies

Char preparation and analyses

Ultimate and proximate analyses of the parent coals are shown in Table 1. Char samples from ten different coals were produced using a fluidized-bed pyrolyzer at 1,273 K. The fluidized bed of MS particles (0.5–0.59 mm) was kept at 1,273 K with nitrogen flowing through at a rate of five times the minimum fluidizing velocity. The coal sample (3g) was introduced from the top of the reactor into the bed. The coal particles were widely and instantaneously spread, and were supplied with heat by the surrounding bed particles; thus, it was estimated that devolatilization took place instantaneously. After keeping the samples in the bed fluidized by nitrogen for about 5 min, the produced char particles were entrained with MS particles through the pipe and collected in the catch pot externally cooled with ice. The char particles collected in the pot were separated from the MS particles by the sink-float separation using the liquids with various densities (water-ethanol mixtures). Details of the pyrolysis method are shown in a previous article (Adschiri et al., 1986). Ash content in char was calculated from the content of ash and fixed carbon in the parent coal, since the amount of volatile matter was found to be negligibly small in char.

The surface areas of N_2 and CO_2 , the active surface area,

and the crystallite size of the graphite structure were measured for some of the chars as shown in Table 2. The CO_2 surface area was evaluated from the isotherm at 298 K by using Polanyi-Dubininn equation. ASA was measured by the same condition used by Radovic et al. (1983). Oxygen chemisorption capacity of chars was determined by using a quartz cell with 0.1 g of chars connected with the vacuum system. After the cell was outgassed at 373 K, a chemisorption experiment was conducted at 375 K and 0.1 MPa air for 12 h. After degasing at 373 K, the char was heated up to 1,225 K at 6 K/min in He stream (30 mL/min), and the temperature was held constant at 1,125 K until all the chemisorbed oxygen was released as CO and CO_2 . Gas analyses were carried out with a gas chromatograph equipped with methanator and flame ionization detector (FID). XRD patterns were obtained for these chars. Crystallite height, L_c , was estimated from the (002) diffraction peak, by using Scherrer equation (Radovic et al., 1983). For these chars, the accurate evaluation of crystallite diameter, L_a , was quite difficult because of the broad peak (10) of diffraction. Since L_c is reported to be a good parameter for correlating gasification rate (Miura, 1989) and L_a has a relation with L_c (Hirsch, 1954, 1958), L_c was employed as a parameter for the chemical structure of char.

Transient kinetics experiment

An experimental apparatus is shown in Figure 1. A quartz tube (6 mm ID) was used as a reactor, which was loaded with 15–85 mg of char (0.5–0.59 mm) and heated up to the desired temperature (1,073–1,273 K) in a pure nitrogen stream (0.5 m/s). The temperature in the bed was measured by a chromel-alumel thermocouple located in the middle part of the bed. The nitrogen stream was switched over to carbon dioxide (0.5 m/s) and gasification was initiated. Effluent gas was sampled intermittently at the intervals of several seconds, and the car-

Table 2. Properties of Char

Coal	N_2 -TSA	CO_2 -TSA	ASA
	m^2/g Carbon in Char		
Yallourn	590	700	152
Baiduri	320	500	162
Taiheiyo	330	330	242
Datong	10	250	70
Hongei	5	100	84

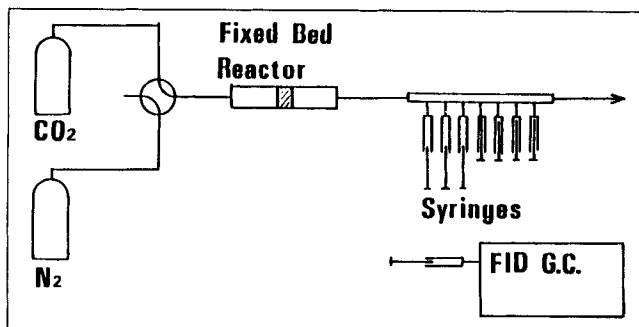


Figure 1. Experimental system of transient kinetic measurement.

bon monoxide concentration, $C_{CO}(t)$, during gasification was analyzed by a gas chromatograph equipped with methanator and FID. Then, the carbon dioxide stream was switched over to nitrogen, and the change of carbon monoxide concentration was monitored intermittently by the same sampling and injection method. Temperature change in the bed immediately after initiating or terminating gasification was not observed under the present experimental conditions. When the carbon monoxide concentration approached zero, carbon dioxide was introduced again. This procedure was repeated several times to cover a wide range of conversion.

A prior experiment was conducted to evaluate the time constant of the system. Carbon dioxide was introduced to the reactor packed with quartz sands (0.5 mm) at 1,173 K and the transient change of carbon dioxide concentration was followed intermittently. After reaching the steady state, the carbon dioxide stream was switched over to nitrogen stream and the transient decay of carbon dioxide concentration was monitored. From this blank test, the time constant of this system was evaluated to be a few seconds.

Analysis

Conversion rates, dX/dt , of chars at several conversion levels were evaluated from the concentration of carbon monoxide, C_{CO} , as follows:

$$\frac{dX}{dt} = \frac{M C_{CO} F}{2 v W_0} \quad (2)$$

where F is the gas flow rate (m^3/s), t is time (s), W_0 is the initial weight of carbon in char (kg), and X is the carbon conversion of char ($\text{kg}_{\text{carbon}}/\text{kg}_{\text{initial carbon}}$). Since the molar weight of carbon, M , is 0.012 (kg/mol) and the molar volume of gas at room temperature, v , is 0.025 (m^3/mol), Eq. 2 is rewritten as Eq. 3.

$$\frac{dX}{dt} = \frac{0.012 C_{CO} F}{2 \times 0.025 W_0} \quad (3)$$

Carbon monoxide concentration, $C_{CO}(t)$, reached the steady state, C_{st} , in several minutes after introducing CO_2 . The dynamic change of $C_{CO}(t)$ was described by the following equation:

$$C_{CO}(t) - C_{st}(t) = [C_{CO}(0) - C_{st}(0)] \exp(-k_{in}t) \quad (4)$$

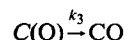
where $C_{st}(t)$ at small t was evaluated by the extrapolation from $C_{st}(t)$ at large t .

The amount of "working active sites," n_w [$\text{mol}/\text{mol}_{\text{initial carbon}}$], was defined as the integrated amount of carbon monoxide evolved after shutting off carbon dioxide, as follows:

$$n_w = \int_0^\infty \frac{0.012 C_{CO} F}{0.025 W_0} dt \quad (5)$$

The value of n_w was evaluated at several conversion levels for the ten different chars. Carbon monoxide produced after shutting off carbon dioxide was attributed to the desorption of surface oxide complex.

Step b:



However, as reported previously (Zhu et al., 1988, 1989), the variation of $C_{CO}(t)$ with time could not be expressed by a simple first-order reaction [$C_{CO}(0) \exp(-kt)$]. Thus, a distribution, $E(k)$, was introduced for k . In this study, the following distribution was employed, because of the fairly good correlation with $C_{CO}(t)$.

$$E(k) = \exp(-k/k_{av})/k_{av} \quad (6)$$

The evolution rate of carbon monoxide after shutting off carbon dioxide is expressed as follows:

$$\frac{C_{CO} F}{0.025} = \frac{n_w W}{0.012} \int_0^\infty k E(k) \exp(-kt) dk \quad (7)$$

$$= \frac{n_w W}{0.012 k_{av}} \int_0^\infty k \exp(-(1 + k_{av}t)k/k_{av}) dk \quad (8)$$

Therefore, the following equation is obtained, by which the variation of $C_{CO}(t)$ with time was analyzed.

$$C_{CO}(t) = C_{CO}(0) (1 + k_{av}t)^{-2} \quad (9)$$

Results and Discussion

Dynamic change in gasification rate

Figure 2 shows the dynamic change of conversion rate with increasing conversion obtained at 1,173 K and 0.1 MPa. Difference in conversion rates of chars were around two orders of magnitude. Change in the conversion rate differs significantly among these ten chars. This is attributed to the physical change of the pore structure of char (Adschiri and Furusawa, 1986) and change in char reactivity. To evaluate the effect of the amount of working active sites, n_w , and the average desorption rate constant, k_{av} , on the variation of the conversion rate, both n_w and k_{av} were evaluated at several conversion levels for the ten different chars. Figure 3 shows the conversion rate per unit number of working active sites, $dX/dt/n_w$. Variation in the rate constant, k_{av} , with increasing conversion is shown in Figure 4. These results suggest that reactivity of char remained mostly constant during gasification, while the gasification rate changed significantly with increasing conversion. Our previous result (Nozaki et al., 1990) indicates that the rate

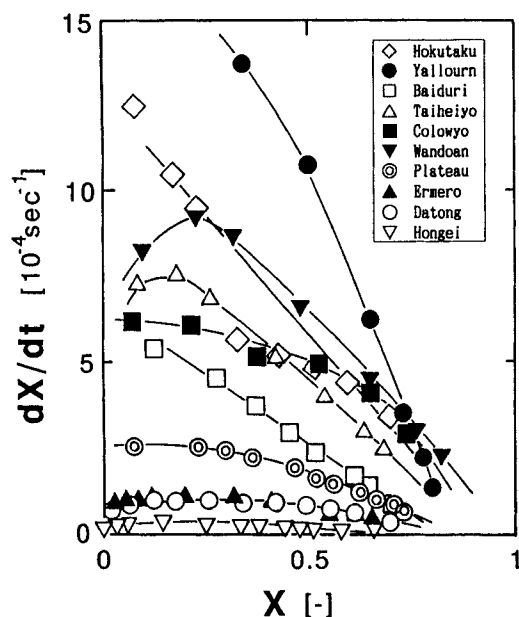


Figure 2. Dynamic change of conversion rate with conversion at 1,173 K and $P_{\text{CO}_2} = 0.1$ MPa.

constant, k_{in} , evaluated for five different chars, was also constant during gasification. Thus, the variation in the gasification rate is attributed to the change of n_w .

According to the reactivity distribution of active sites, the gasification rate can be expressed as follows:

$$\frac{dX}{dt} = \frac{0.012 C_{\text{CO}} F}{2 \times 0.025 W_0} = n_w \int_0^\infty kE(k) dk \quad (10)$$

$$\frac{dX}{dt} = n_w k_{av} \quad (11)$$

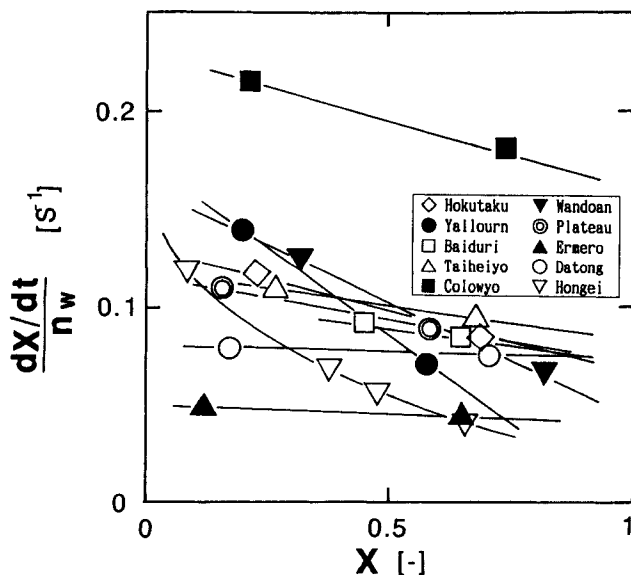


Figure 3. Conversion rate per unit amount of working active sites at the conversion level of 1,173 K, $P_{\text{CO}_2} = 0.1$ MPa.

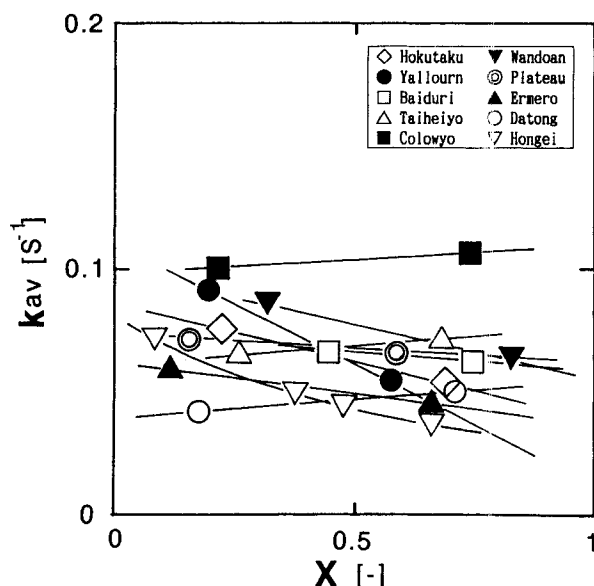


Figure 4. Rate constant, k_{av} , at the conversion level of 1,173 K, $P_{\text{CO}_2} = 0.1$ MPa.

Therefore, $dX/dt/k_{av}$ should be equal to n_w . Figure 5 shows that these values agree fairly well. The result supports the validity of the present analysis. Since the difference in k_{av} among chars shown in Figure 4 is not great, the result shown in Figure 5 implies that around 100 times in the difference of the gasification rate among chars can be explained mostly by the difference in n_w , as discussed in detail in the following section.

Difference in gasification rate

The effects of partial pressure of CO_2 on k_{av} and k_{in} at 1,123 K for five different chars are shown in Figures 6 and 7. The differences in the rate constant among chars were found to be small at this temperature. The value of k_{in} increased with in-

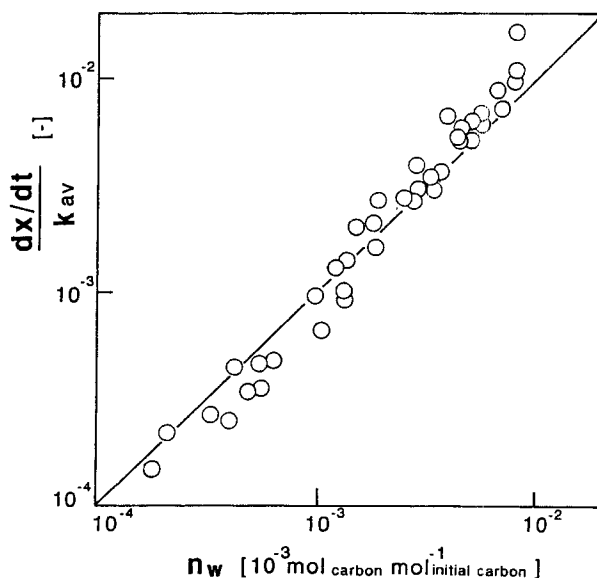


Figure 5. Relation between $dX/dt/k_{av}$ and n_w .

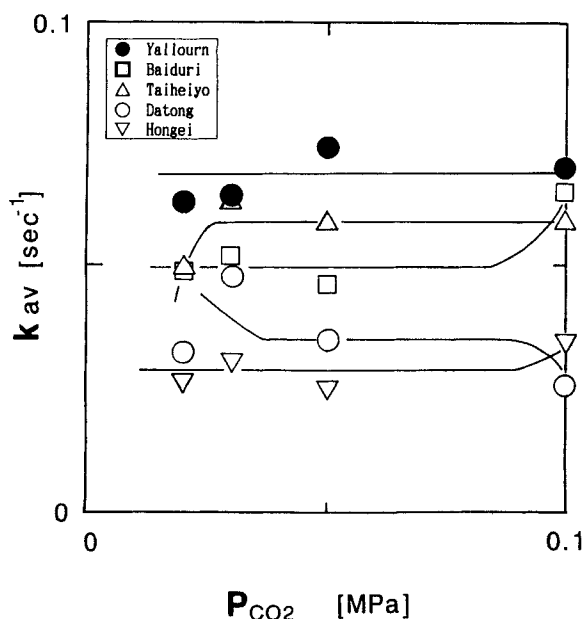


Figure 6. Partial pressure effect of CO_2 on k_{av} at 1,123 K.

creasing partial pressure of CO_2 , while k_{av} remained mostly constant.

If there is no reactivity distribution, k_{in} is described as $(k_3 + k_1 P_{\text{CO}_2})$ and k_{av} is k_3 , according to Ergun's mechanism. Therefore, the intercept of k_{in} vs. P_{CO_2} plot should be equal to the value of k_{av} . The result shown in Figures 6 and 7 did not clearly indicate the relation. Assumed that this is due to the activity distribution of carbon.

Figure 8 shows the conversion rate at the conversion level of 0.5 for ten chars. The desorption rate constants evaluated over a wide range of temperatures are shown in Figure 9. Difference in conversion rate shown in Figure 8 was about 100 times, but the difference in k_{av} was less than 3 times. The value of k_{av} increases with decreasing carbon content in parent coal. This difference may be due to the difference in the chemical structure of char. Figure 10 shows the relation between the conversion rate and the amount of working active sites. The good linear relation suggests that the difference in the gasi-

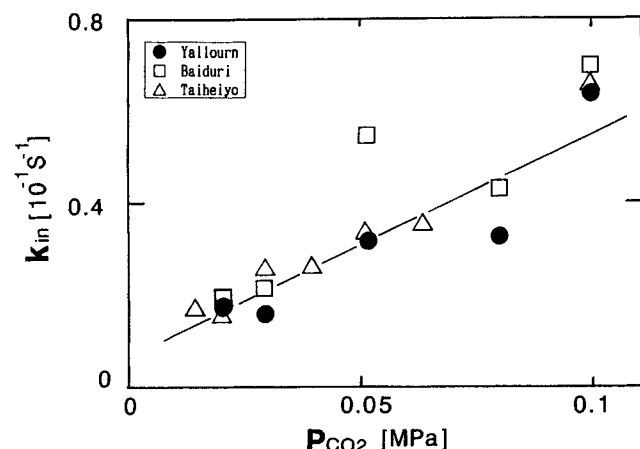


Figure 7. Partial pressure effect of CO_2 on k_{in} at 1,123 K.

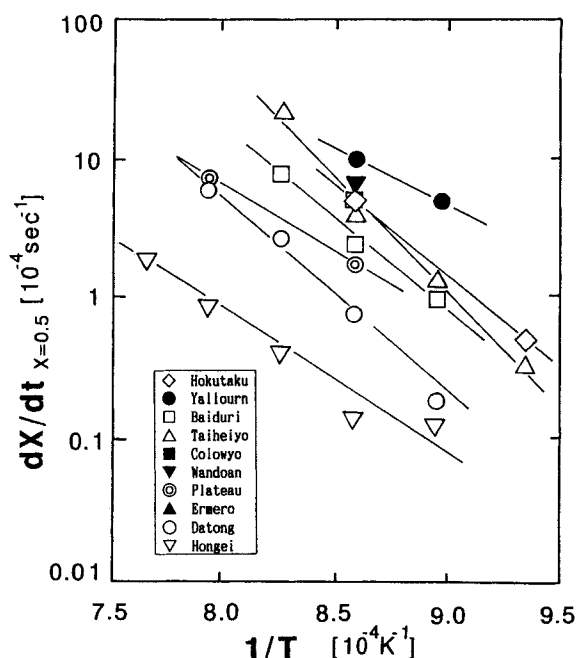


Figure 8. Arrhenius plot of conversion rate at the carbon conversion level of 0.5.

fication rate may be due largely to the difference in the amount of working active sites.

The activation energy of observed gasification rate ranged from 150 to 240 kJ/mol for these coals, while that of k_{av} is approximately 125 kJ/mol. This implies that the number of working active sites depends on the temperature.

Huttinger and Nill (1990) used the rapid cooling method to evaluate the number of working active sites during gasification of pure carbon over a wide range of temperatures. They reported that the activation energy of n_w , E_0 , was -125 kJ/mol by assuming the following relation.

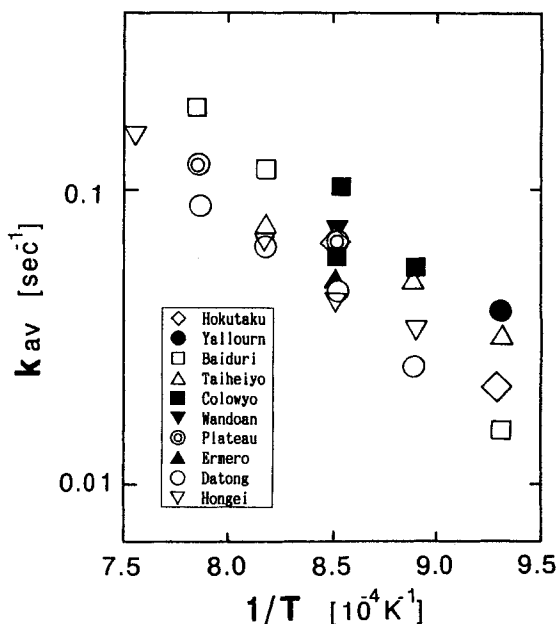


Figure 9. Arrhenius plot of k_{av} .

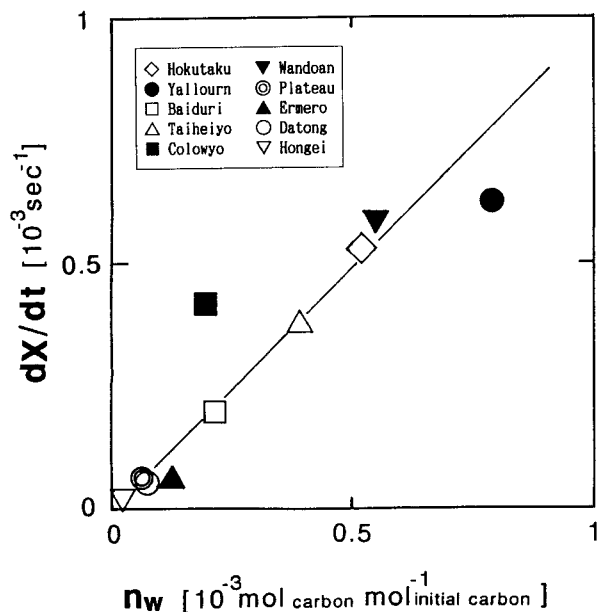


Figure 10. Amount of working active sites vs. conversion rate at 1,173 K.

$$\text{Observed gasification rate} = k_0 \exp(-E_k/RT) \times n_w \exp(-E_0/RT) \quad (12)$$

where $k_0 \exp(-E_k/RT)$ is the desorption rate constant, and the temperature dependence is described as $n_w \exp(-E_0/RT)$.

Equation 12 shows that the difference between the activation energy (20–115 kJ/mol) and the gasification rate, k_{av} in the present study may be due to E_0 . However, in this case, E_0 has a positive value. E_0 of the pure carbon reported by Huttlinger and Nell (1990) differs from that of these chars due probably

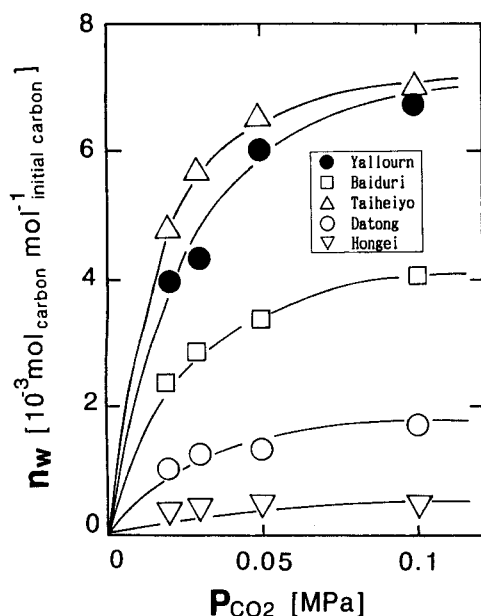


Figure 11. Partial pressure effect of CO₂ on the amount of working active sites at 1,123 K.

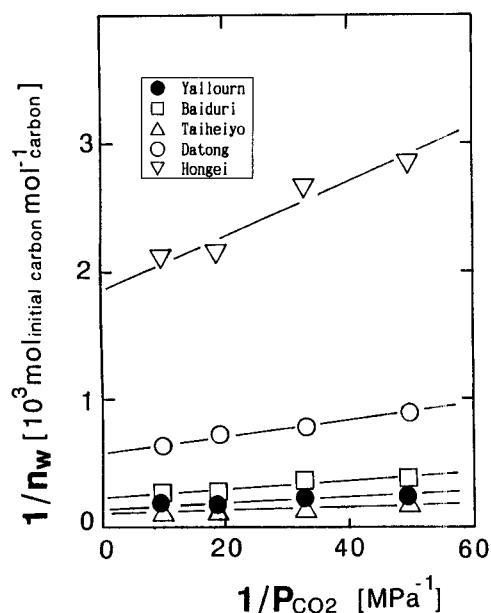


Figure 12. Amount of working active sites vs. partial pressure of CO₂ at 1,123 K.

to the differences of the method used for the evaluation of n_w , reactivity of carbon, and the activity distribution of active sites.

Relation between total number of active site and carbon structure

The effect of partial pressure of CO₂ on n_w was examined, Figure 11. The number of working active sites increased and tended to approach a maximum value, N , with increasing partial pressure of CO₂.

To evaluate the maximum value, N , Langmuir-type pressure dependence was assumed.

$$n_w = \frac{NKP_{CO_2}}{1 + KP_{CO_2}} \quad (13)$$

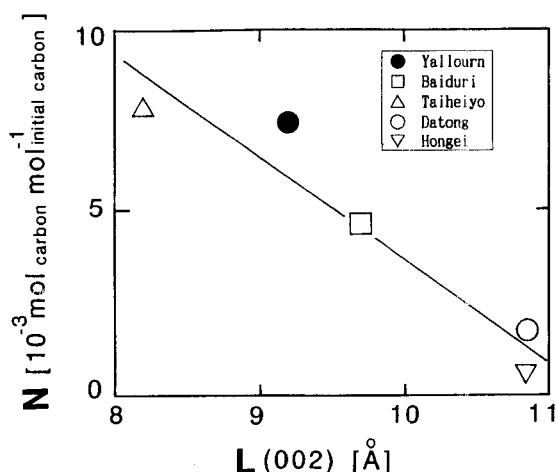


Figure 13. Total amount of active sites, N , vs. crystallite size of graphite structure in char, L .

Ergun's mechanism (Ergun, 1956), which assumes the steady-state condition and negligible reverse reaction ($C(O) + CO \rightarrow C + CO_2$), offers:

$$\frac{dn_w}{dt} = k_1 P_{CO_2} (1 - \theta) N_T - k_3 \theta N_T = 0 \quad (14)$$

where N_T is the number of active sites, and θ is the occupied fraction of active sites by surface oxide complex. Therefore, the number of working active sites is described as:

$$n_w = \frac{N_T k_1 P_{CO_2} / k_3}{1 + k_1 P_{CO_2} / k_3} \quad (15)$$

By considering the distribution of rate constants, a more complicated formula is derived. However, in this analysis Eq. 13 was employed to express the pressure dependence on n_w . $1/n_w$ was plotted against $1/P_{CO_2}$ in Figure 12; fairly good linear relation was obtained. From the intercept of this line, N was evaluated by using Eq. 16, which is rearranged from Eq. 13.

$$\frac{1}{n_w} = \frac{1}{K N P_{CO_2}} + \frac{1}{N} \quad (16)$$

Relation between N and the physical property of char was investigated. The maximum value, N , tends to increase with decreasing carbon content of parent coal. Table 2 shows some properties of chars. Char, whose surface area is large, has the high value of N . Figure 13 shows the relationship between N and the crystallite size of graphite in char. The value of N increases with decreasing crystallite size of the graphite structure of carbon. We assumed that this maximum value, N , is closely related to the total number of active sites, N_T , namely the carbon structure of char.

A well-developed graphite structure has large L_a and small L_c (Radovic et al., 1983). Radovic et al. (1983) concluded that the active site for gasification is the edge carbon of graphite plane by analyzing the relationship between the gasification rate and the graphite size of char (L_a and L_c). The relation between N and L_c shown in Figure 13 suggests that a large graphite structure has less active sites. Thus, the same conclusion as Radovic et al. can be deduced from the result. We think that the distribution of the reactivity of active site is attributed to the distribution of graphite structure (L_c and L_a) and the effect of amorphous carbon in chars. The detailed analysis on the relation between N and carbon structure is required in a future research.

Conclusion

The transient kinetics method was applied effectively to the evaluation of both rate constants, k_{av} and k_m , and the amount of working active sites, n_w . k_{av} and k_m were almost the same for the ten chars employed and remained mostly constant during reaction. Thus, the difference in CO_2 gasification rates of ten chars was explained by the difference in n_w . The amount of working active sites, n_w , increased with increasing carbon dioxide concentration and tended to approach a maximum value, N . The maximum value, N , was considered as the total number of active sites and was closely related to the carbon structure of char, especially to the crystallite size of graphite.

From those results, differences in gasification rates among chars can be attributed to the difference in N , rather than in the elemental rate constants.

Acknowledgment

The authors wish to express sorrow over the passage of Professor Furusawa before the completion of this work. T. A. gratefully acknowledges support for this research by a Grant-in-Aid for Energy Research (63603014 and 01603012).

Notation

- C_{CO} = carbon monoxide concentration, mol/mol
- C_{CO_2} = carbon dioxide concentration, mol/mol
- E = distribution function, s
- F = gas flow rate, m^3/s
- K = equilibrium constant, L/Pa
- k_1 = elemental rate constant, L/Pa/s
- k_2 = elemental rate constant, L/Pa/s
- k_3 = elemental rate constant, L/s
- k_m = time constant of the transient response during initiating gasification, L/s
- k_{av} = average value of time constant of the transient response after terminating gasification, L/s
- L = crystallite size of graphite structure of char, A
- N = total amount of active sites, mol/mol_{initial carbon}
- N_w = number of active sites, mol/mol_{initial carbon}
- n_w = number of working active sites, mol/mol_{initial carbon}
- P = partial pressure, Pa
- t = time, s
- W_0 = initial weight of carbon in char, kg
- X = carbon conversion, kg_{carbon}/kg_{initial carbon}

Literature Cited

- Adschiri, T., T. Shiraha, K. Ogawa, and T. Furusawa, "Unified Interpretation of CO_2 and Steam Gasification Rates of Coal Chars by Use of Surface Area," *Proc. Int. Conf. on Coal Sci.*, 289 (1985).
- Adschiri, T., and T. Furusawa, "Relation between CO_2 Reactivity of Coal Char and BET Surface Area," *Fuel*, 65, 927 (1986).
- Adschiri, T., T. Shiraha, T. Kojima, and T. Furusawa, "Prediction of CO_2 Gasification Rate of Char in Fluidized Bed Gasifier," *Fuel*, 65, 1688 (1986).
- Blyholder, G., J. S. Binford, and H. Eyring, "A Kinetic Theory for the Oxidation of Carbonized Filaments," *J. Phys. Chem.*, 62, 263 (1958).
- Cerfontain, R., "Alkali Catalyzed Carbon Gasification," PhD Thesis, Institute for Chemical Technology, University of Amsterdam (1986).
- Cerfontain, R., R. Meijer, F. Kapteijn, and J. A. Moulijn, "Alkali-Catalyzed Carbon Gasification in CO/CO_2 Mixtures: an Extended Model for the Oxygen Exchange and Gasification Reaction," *J. Catal.*, 107, 173 (1987).
- Ergun, S., "Kinetics of Reaction of Carbon Dioxide with Carbon," *J. Phys. Chem.*, 60, 480 (1956).
- Freund, H., "The Kinetics of Carbon Gasification by CO_2 ," *ACS Div. Fuel Chem.*, 311 (1985).
- Freund, H., "Gasification of Carbon by CO_2 : a Transient Kinetics Experiment," *Fuel*, 65, 63 (1986).
- Hashimoto, K., K. Miura, J.-J. Xu, A. Watanabe, and H. Masukami, "Relation between the Gasification Rate of Carbons Supporting Alkali Metal Salts and the Amount of Oxygen Trapped by the Metal," *Fuel*, 65, 489 (1986).
- Hashimoto, K., K. Miura, and J. J. Xu, "Investigation of Alkali Metal Catalyzed Carbon-Steam and Carbon- CO_2 Reaction by Use of the Flash Desorption Technique," *Proc. Int. Conf. on Coal Science*, Elsevier, Amsterdam, 523 (1987).
- Hirsch, P. B., "Conclusion from X-Ray Scattering Data on Vitrain Coals," *Proc. Res. Conf. on Science in the use of Coal*, Scheffeld, A29 (1958).
- Hirsch, P. B., "X-Ray Scattering from Coals," *Proc. Roy. Soc., London*, A226, 143 (1954).

- Huttinger, K. J., and J. S. Nill, "A Method for the Determination of Active Sites and True Activation Energy in Carbon Gasification: II. Experimental Results," *Carbon*, **28**, 457 (1990).
- Jiang, H., and L. R. Radovic, "Transient Kinetic Studies of Char Gasification in Carbon Dioxide," (ACS) Div. Fuel Chemistry, 79 (1989).
- Kasaoka, S., and Y. Sakata, S. Kayano, and Y. Masuoka, "Kinetic Evaluation of the Reactivity of Various Coal Chars for Gasification with Carbon Dioxide in Comparison with Steam," *Kagaku-Kogaku Ronbunshu*, **8**, 174 (1982); *Inter. Chem. Eng.*, **25**, 160 (1985).
- Laine, N. R., F. J. Vastola, and P. L. Walker, "The Importance of Active Surface Area in the Carbon-Oxygen Reaction," *J. Phys. Chem.*, **67**, 2030 (1963).
- Lizzio, A. A., H. Jiang, and L. R. Radovic, "On the Kinetics of Carbon (Char) Gasification: Reconciling Models with Experiments," *Carbon*, **28**, 7 (1990).
- Mims, C. A., and J. K. Pabst, "Role of Surface Salt Complexes in Alkali-Catalysed Carbon Gasification," *Fuel*, **62**, 176 (1983).
- Nagle, J., and R. F. Strickland-Constable, "Oxydation of Carbon between 1,000–2,000°C," *Proc. Conf. Carbon*, Vol. 1, Pergamon Press, New York, 154 (1963).
- Nozaki, T., T. Adschiri, and T. Furusawa, "Characterization of Coal Char Reactivity by Transient Kinetic Technique," *Fuel Proc. Technol.*, **24**, 277 (1990).
- Radovic, L. R., P. L. Walker, Jr., and R. G. Jenkins, "Importance of Carbon Active Sites in the Gasification of Coal Chars," *Fuel*, **62**, 849 (1983).
- Radovic, L. R., K. Steczko, P. L. Walker, and R. G. Jenkins, "Combined Effect of Inorganic Constituents and Pyrolysis Conditions on the Gasification Reactivity of Coal Chars," *Fuel Proc. Technol.*, **10**, 311 (1985).
- Saber, J. M., J. L. Falconer, and L. F. Brown, "Interaction of Potassium Carbonate with Surface Oxides of Carbon," *Fuel*, **65**, 1356 (1986).
- Saber, J. M., K. B. Kester, J. L. Falconer, and L. F. Brown, "A Mechanism for Sodium Oxide Catalyzed CO₂ Gasification of Carbon," *J. Catal.*, **109**, 329 (1988).
- Sams, D. A., and F. Shadman, "Mechanism of Potassium-Catalyzed Carbon/CO₂ Reaction," *AIChE J.*, **32**, 1132 (1986).
- Smith, I. W., "The Intrinsic Reactivity of Carbons to Oxygen," *Fuel*, **57**, 409 (1978).
- Takeda, S., K. Kitano, J. Kubota et al., "Effect of Coal Nature on Intrinsic Reaction Rate of Coal Char Gasification by CO₂," *J. Fuel Soc. Japan*, **64**, 409 (1985).
- Zhu, Z.-B., T. Adschiri, and T. Furusawa, "Evaluation of Intrinsic CO₂ Gasification Rate of Coal Char and Number of Active Site during Gasification by Use of Transient Kinetics Experiments," *Proc. Int. Conf. on Coal Science*, J. A. Moulijn et al. ed., Elsevier, Amsterdam-Oxford-New York-Tokyo, 515 (1987).
- Zhu, Z.-B., T. Adschiri, and T. Furusawa, "Evaluation of Both Intrinsic Reaction Rate and Number of Active Sites in Carbon Dioxide Gasification of Coal Char," *Proc. Japan-China Symp. on Coal and Cl Chemistry*, Y. Tamai et al., ed., Tokyo, Japan (May 9–11, 1988).
- Zhu, Z.-B., T. Furusawa, T. Adschiri, and T. Nozaki, "Characterization of Coal Char Reactivity by the Number of Active Sites during CO₂ Gasification," *ACS Div. Fuel Chem.*, **87** (1989).

Manuscript received Nov. 2, 1990, and revision received Mar. 27, 1991.